J Biomol NMR (2012) 54:337–342
DOI 10.1007/s10858-012-9687-5

COMMUNICATION

GFT projection NMR for efficient $^{1}H/^{13}C$ sugar spin system identification in nucleic acids

Hanudatta S. Atreya · Bharathwaj Sathyamoorthy · Garima Jaipuria · Victor Beaumont · Gabriele Varani · Thomas Szyperski

Received: 25 September 2012 / Accepted: 16 November 2012 / Published online: 29 November 2012

Abstract A newly implemented G-matrix Fourier transform (GFT) (4,3)D HC(C)CH experiment is presented in conjunction with (4,3)D HCCH to efficiently identify $^{1}H/^{13}C$ sugar spin systems in ^{13}C labeled nucleic acids. This experiment enables rapid collection of highly resolved relay 4D HC(C)CH spectral information, that is, shift correlations of ^{13}C–^{1}H groups separated by two carbon bonds. For RNA, (4,3)D HC(C)CH takes advantage of the comparably favorable 1′- and 3′-CH signal dispersion for complete spin system identification including 5′-CH. The (4,3)D HC(C)CH/HCCH based strategy is exemplified for the 30-nucleotide 3′-untranslated region of the pre-mRNA of human U1A protein.

Keywords GFT projection NMR · Nucleic acids · Resonance assignment · RNA

Abbreviations

GFT	G-matrix Fourier transformation
r.f.	Radio-frequency
RNA	Ribonucleic acid

The resonance assignment of nucleic acids is a prerequisite for their three-dimensional (3D) structure determination and depends critically on the sugar spin system identification (Varani et al. 1996). For nucleic acid molecules with more than about 15 nucleotides, $^{13}C/^{15}N$-labeling is often required for resonance assignment based on heteronuclear NMR spectroscopy. Such stable isotope labeling can be accomplished either enzymatically (Nikonowicz et al. 1992; Pardi 1992; Batey et al. 1992, 1995; Varani et al. 1995, 1996; Price et al. 1998; Masse et al. 1998) or by use of solid-phase synthesis for DNA (Kojima et al. 2001). The ^{1}H and ^{13}C resonance assignment of the sugar resonances not only provides an increased number of ^{1}H–^{1}H upper distance limit constraints obtained from heteronuclear resolved nuclear Overhauser enhancement spectroscopy (NOESY), but also allows one to derive (1) dihedral angle constraints from $^{3}J_{HH}$ scalar couplings measured in ^{13}C-resolved in-phase [^{1}H,^{1}H]-COSY (Grzesiek et al. 1995) for studying sugar conformations (Varani and Tinoco 1991; Szyperski et al. 1998; Fernández et al. 1999), (2) dihedral angle constraints from $^{3}J_{CP}$ and $^{3}J_{HP}$ couplings measured (Pardi 1992; Legault et al. 1995; Marino et al. 1994; Schwalbe et al. 1995; Varani et al. 1995, 1996; Ramachandran et al. 1996; Szyperski et al. 1997; Hoogstraten and Pardi 1998; Szyperski et al. 1999) to constrain the conformation of the phosphate backbone (Pardi 1992; Varani et al. 1995, 1996; Szyperski et al. 1997, 1999), and

Electronic supplementary material The online version of this article (doi:10.1007/s10858-012-9687-5) contains supplementary material, which is available to authorized users.

H. S. Atreya · G. Jaipuria
NMR Research Centre, Indian Institute of Science, Bangalore 560012, India

B. Sathyamoorthy · V. Beaumont · T. Szyperski (✉)
Department of Chemistry, State University of New York at Buffalo, Buffalo, NY 14260, USA
e-mail: szypersk@buffalo.edu

G. Varani
Department of Chemistry, University of Washington, Seattle, WA 98195, USA

G. Varani
Department of Biochemistry, University of Washington, Seattle, WA 98195, USA

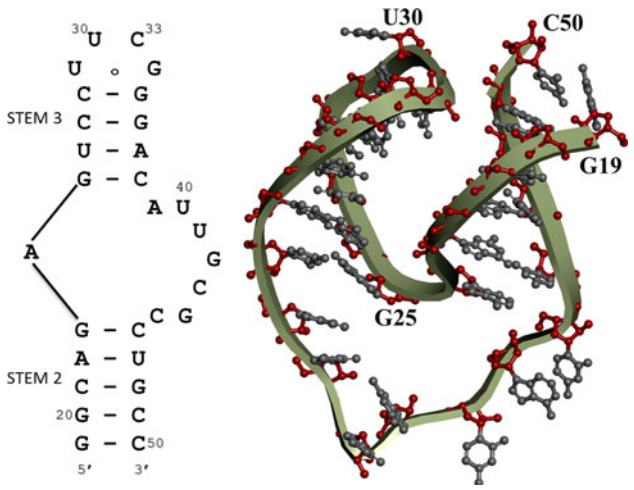

Fig. 1 Secondary structure (*on the left*) and tertiary structure (*on the right*) of the 30-nucleotide binding site within the 3′-untranslated region of the pre-mRNA encoding U1A protein, from previous NMR studies by (Gubser and Varani 1996) Note that C31 and C32 within the wild-type RNA sequence were deleted). On the *right*, the phosphate backbone is represented by a *ribbon*, and the sugar and bases are represented as *ball and sticks colored in red and grey*, respectively. The positions of the 5′ and 3′ terminal nucleotides G19 and C50, of U30 located immediately upstream to the deletion, while G25, for which NMR signals are shown in Fig. 4, is labeled. The GFT NMR experiments presented in this paper enabled nearly complete spin system identification of the sugar resonances

(3) orientational constraints from residual dipolar ^{13}C–^{1}H couplings to refine the structure (e.g. Bayer et al. 1999; Wu et al. 2003).

3D HCCH (e.g. Nikonowicz and Pardi 1993; Latham et al. 2005) and H(CC)CH (Nikonowicz and Pardi 1993) experiments are most popular for sugar spin system identification. Furthermore, 4D HCCH can provide the four-dimensional spectral information which is often required to resolve the shift degeneracy encountered for ribose spins in RNA. However, the associated long minimal measurement times result in sampling limited data acquisition (Szyperski et al. 2002). The same holds for hypothetical 4D HC(C)CH yielding 'relayed' shift correlations of ^{13}C–^{1}H groups separated by two carbon bonds.

G-matrix FT (GFT) projection NMR spectroscopy (Kim and Szyperski 2003; Atreya and Szyperski 2004, 2005, 2006) enables to rapidly obtain highly resolved, high-dimensional NMR spectral information so that sampling limited data acquisition can be avoided. Moreover, GFT NMR solely relies on the linear combination of time domain data which are then Fourier transformed. Hence, in contrast to other approach for sparse time domain sampling (Kazimierczuk and Orekhov 2011; Holland et al. 2011; Hyberts et al. 2012; Mobli et al. 2012) employment of a non-linear algorithm to reconstruct frequency domain spectra is not required. In this communication, we present a strategy for the identification of sugar spin systems in nucleic acids based on GFT (4,3)D HC(C)CH/HCCH, where (4,3)D indicates a reduction of dimensionality from 4D to 3D and the underlined letters indicate the nuclei for which the chemical shift evolution periods are jointly sampled (Kim and Szyperski 2003; Atreya and Szyperski 2005). The strategy was exemplified for the 30-nucleotide binding site of human U1A protein within the 3′-untranslated region of its pre-mRNA (Gubser and Varani 1996; Fig. 1): the constant-time 2D [^{13}C,^{1}H] HSQC spectrum (Santoro and King 1992; Vuister and Bax 1992) exhibits the characteristically limited chemical shift dispersion of the sugar resonances observed for RNA (Fig. 2) where (nearly) complete identification of sugar spin systems can evidently greatly benefit from 4D HCCH and HC(C)CH spectral information.

The radiofrequency (r.f.) pulse scheme of sensitivity enhanced (Kay et al. 1992) (4,3)D HC(C)CH is shown in Fig. 3. A scheme without sensitivity enhancement may be preferred for very large RNA molecules and is provided in Fig. S1 of the Supplementary Material along with corresponding implementations of (4,3)D HCCH (Figs. S2 and S3). When compared with (4,3)D HCCH, an additional ^{13}C–^{13}C polarization transfer step is introduced for (4,3)D HC(C)CH (Table 1). Frequency labeling on the first and third ^{13}C spin then results in the desired shift correlations of ^{13}C–^{1}H moieties separated by two carbon bonds. Product operator calculations (Cavanagh et al. 2007; see Supplementary Material) performed using the program POMA (Güntert et al. 1993; Güntert 2006) yield the dependence of the ^{13}C–^{13}C polarization transfer amplitudes (Table S1) on the constant time delay T (legend of Fig. 3), and thus approximate relative peak intensities. In turn, this allows tuning of the delay T to $\sim 1/3.125 * J_{CC}$ ($J_{CC} = 40$ Hz) such that the relative intensities of the desired HCCH and HC(C)CH relay peaks are both about equally intense (note that for uniform ^{13}C T_2 relaxation times the ratios of the amplitudes of HCCH and HC(C)CH relay peaks are not affected; see Supplementary Material).

Phase sensitive joint sampling of ^{1}H and ^{13}C chemical shifts in the GFT dimension is accomplished by co-incrementing their respective chemical shift evolution periods where ^{1}H shift evolution can be scaled (by a factor 'κ'; Fig. 3) relative to ^{13}C (Kim and Szyperski 2003; Szyperski and Atreya 2006) to adjust signal dispersion and/or to minimize signal loss due to transverse ^{1}H-relaxation and passive ^{1}H–^{1}H scalar couplings. For the same reason, evolution of ^{1}H shifts is implemented in a semi-constant time manner (Grzesiek and Bax 1993). G-matrix transformation results in two sub-spectra comprising of peaks at ω_1:$\Omega(^{13}C) \pm \kappa * \Omega(^{1}H)$, and 3D (H)C(C)CH (recorded with the pulse scheme of Fig. 3 while omitting the ^{1}H chemical shift evolution during t_1) yields central peaks at ω_1:$\Omega(^{13}C)$.

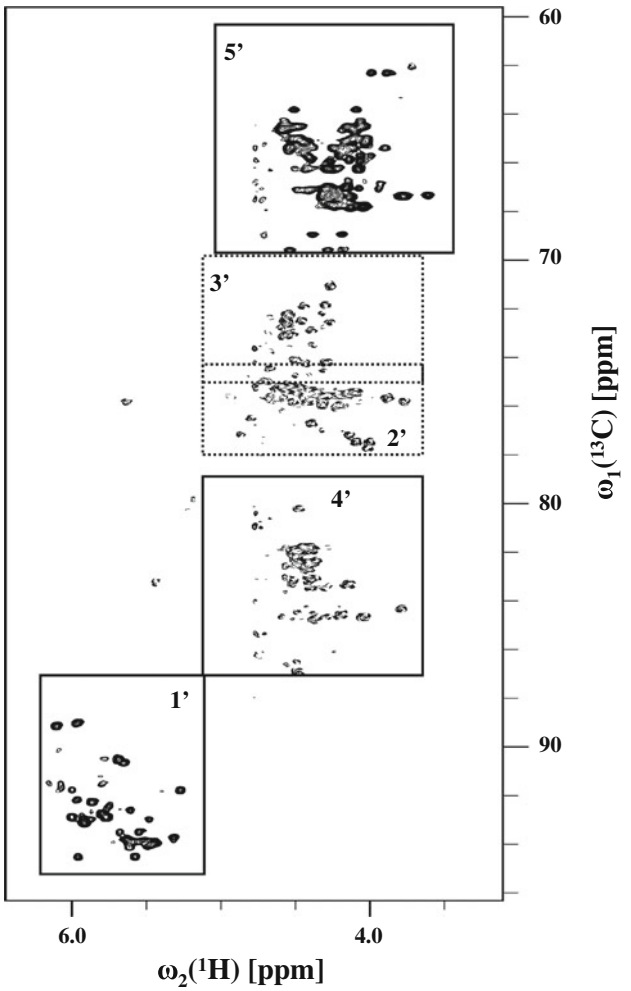

Fig. 2 Constant-time 2D [^{13}C,^{1}H] HSQC spectrum recorded in 45 min at 25 °C and a ^{1}H resonance frequency of 750 MHz for the ~1 mM solution of the 30-nucleotide RNA molecule of Fig. 1. Spectral regions containing peaks arising from given ^{13}C–^{1}H sugar resonances are indicated and boxed

The new experiment (Fig. 3) enables rapid recording of highly resolved 4D HC(C)CH spectral information. (4,3)D HC(C)CH was acquired along with (4,3)D HCCH as described in Eletsky et al. (2005) but with delays adapted for nuclei acids (Figs. S2, S3) for a 1.0 mM solution of the U–^{13}C/^{15}N labeled 30-nucleotide 3′-untranslated region of pre-mRNA of protein U1A dissolved in 100 % $^{2}H_2O$ containing 10 mM phosphate buffer at pH = 6 (Gubser and Varani 1996; sequence GGCAGAGUCCUUCGG GACAUUGCACCUGCC). The spectra were acquired (Table 2; relaxation delay between scans: 1 s) at 25 °C on a Varian INOVA 750 spectrometer equipped with a conventional ^{1}H{^{13}C,^{15}N} probe. Since acquisition parameters were matched to enable efficient combined interactive spectral analysis, the measurement times were 15 h for both (4,3)D HC(C)CH and (4,3)D HCCH (Table 2). The factor scaling ^{1}H relative to ^{13}C shift evolution (Fig. 3) was set to $\kappa = 1$, so that ω_1:Ω(^{13}C) ± Ω(^{1}H) was measured along the GFT dimension. The spectra were processed using NMRPipe (Delaglio et al. 1995) and analyzed using XEASY (Bartels et al. 1995).

Figure 4 shows composite plots of [ω_1(^{13}C;^{1}H),ω_3(^{1}H)]-strips taken from relay (4,3)D HC(C)CH and (4,3)D HCCH to exemplify the spin system identification for the ribose moiety of G25. Comparison of signals observed in the two (4,3)D experiments renders straightforward the peak identification starting with the ^{13}C–^{1}H shift correlations observed in 2D [^{13}C,^{1}H] HSQC (Fig. 2). Importantly, (4,3)D HC(C)CH directly correlates comparably well resolved 1′- and 3′-CH shifts through relayed peaks which are not registered in (4,3)D HCCH. Hence, in contrast to (4,3)D HCCH, the correlation of 1′- and 3′-CH shifts is not impeded by 2′-CH shift degeneracy. Furthermore, (4,3)D HC(C)CH allows (1) validation of 2′ and 4′-CH shifts obtained from (4,3)D HCCH by detection of relay 2′ and 4′-CH peaks, and (2) the advantage of the comparably well resolved 3′-CH shifts to correlate with 5′-CH shifts. Specifically, 5′-CH shifts can be efficiently measured by locating relay peaks at ω_1:Ω(^{13}C5′) ± Ω(^{1}H5′) or ω_1:Ω(^{13}C5″) ± Ω(^{1}H5″) and [ω_2:Ω(^{13}C3′);ω_3:Ω(^{1}H3′)] after signal detection on ^{1}H3′: in contrast to (4,3)D HCCH, 5′-CH shift assignments are not hampered by 4′-CH shift degeneracy.

(4,3)D HC(C)CH/(4,3)D HCCH readily yielded nearly complete ribose spin system identifications (97 % of all ^{1}H and ^{13}C shifts have been measured; Table S2) for the 30-nucleotide RNA of the present study (Gubser and Varani 1996; Fig. 1). The near completeness of ribose spin system identification reflects the high yield of resolved peaks detected on CH-moieties other than C5′H: 89 % (160 of 180)/88 % (212 of 240) of the expected relay peak/cross peaks were detected and resolved, respectively, in (4,3)D HC(C)CH/(4,3)D HCCH. In fact, the (4,3)D HC(C)CH spectrum alone correlated according to spin system all chemical shifts that were previously obtained (Gubser and Varani 1996). Further, we measured the average signal-to-noise (S/N) values for the different types of peaks (Table S1). First, this analysis showed that relative peak intensities are in agreement with product operator calculations (Tables S1). Second, it revealed that the measurement time of 15 h employed for (4,3)D HC(C)CH was adequate to obtain workable S/N ratios for an RNA molecule of about 10 kDa even without use of a cryogenic probe. Hence, the acquisition of the conventional 4D congener would have been highly sampling limited (the corresponding measurement times with minimal spectral widths but the same maximal chemical shift evolution times is about 5 days). In fact, the higher sensitivity of (4,3)D HCCH when compared with (4,3)D HC(C)CH would have allowed us to further cut back its measurement time by, for example, single-scan

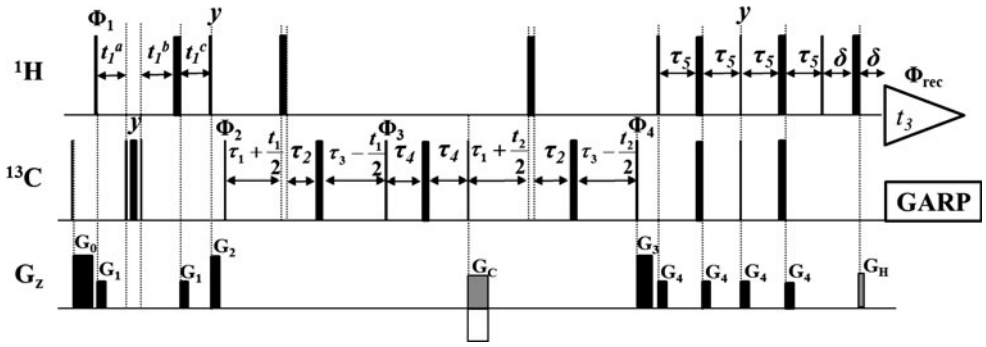

Fig. 3 R.f. pulse scheme of sensitivity enhanced relayed (4,3)D HC(C)CH for nucleic acids. *Rectangular* 90° and 180° pulses are indicated by *thin* and *thick vertical bars*, respectively, and *phases* are indicated above the pulses. Where no r.f. phase is marked, the pulse is applied along *x*. High-power 90° pulse lengths are: 5 μs for ^{1}H, 14 μs for ^{13}C. The ^{1}H r.f. carrier is placed at the position of the solvent line at 4.72 ppm. GARP (Shaka et al. 1985) is employed to decouple ^{13}C (r.f. = 2.5 kHz) during signal detection. A $90^{0}_{x} - 180^{0}_{y} - 90^{0}_{x}$ composite pulse (Cavanagh et al. 2007) is used to achieve broadband inversion of ^{13}C during the transfer of polarization from ^{1}H to ^{13}C. The ^{1}H shift evolution during t_1 is implemented in a semi-constant time manner with $t_1^{a}(0) = 1.7$ms, $t_1^{b}(0) = 1\mu$s, $t_1^{c}(0) = 1.7$ms, and $\Delta t_1^{a} = \kappa * t_1/2$, $\Delta t_1^{b} = \Delta t_1^{a} + \Delta t_1^{c}$, $\Delta t_1^{c} = -\kappa * t_1/2t_{1,\max}(^{13}\mathrm{C})$. κ is the scaling factor and was set to 1.0 (see also text). The delays are: $\tau_1 = 1.1$ ms, $\tau_2 = 2.9$ ms, $T/2 = \tau_1 + \tau_2 = \tau_3 = \tau_4 = 4.0$ ms, $\tau_5 = 1.4$ ms and $\delta = 1.0$ ms, with $T = 1/[3.125\ J_{CC}]$ defining the delay for ^{13}C–^{13}C polarization transfer with $J_{CC} = 40$ Hz (see text). In order to observe signals arising from CH– and CH_2–moieties, the $^{1}J_{CH}$-refocussing time for the initial INEPT and the delays of the sensitivity enhancement scheme are set to a 'compromise values' accounting for a passive $^{1}J_{CH}$ coupling in CH_2-moieties (Cavanagh et al. 2007). Pulsed z-field gradients (PFGs) are of rectangular shape, and their duration and strengths are: G_0 (1.0 ms, 13 G/cm); G_1 (0.5 ms, 11 G/cm), G_2 (1 ms, 15 G/cm), G_3(1 ms, 15 G/cm), G_4 (0.5 ms, 11 G/cm), G_C (1.2 ms; 24 G/cm), G_H (0.3 ms; 24 G/cm). Phase cycling: $\Phi_1 = x$; $\Phi_2 = x, -x$; $\Phi_3 = x, -x$; $\Phi_4 = x$; $\Phi_{rec} = x, -x$. Quadrature detection in $t_2(^{13}\mathrm{C})$ is achieved with sensitivity enhancement (Kay et al. 1992; G_C is inverted with a 180° shift for Φ_4) and in $t_1(^{13}\mathrm{C};^{1}\mathrm{H})$, Φ_2 is altered according to States-TPPI (Cavanagh et al. 2007). The GFT NMR phase-cycle (Kim and Szyperski 2003) is $\Phi_1 = x, y$

Table 1 Polarization transfer in (4,3)D HCCH and HC(C)CH experiments

Magnetization transfer pathways	Linear combinations of shifts in GFT dimension (ω_1)
(4,3)D HCCH	$\Omega(^{13}\mathrm{C}^{(a)}) \pm \Omega(^{1}\mathrm{H}^{(a)})$
$^{1}\mathrm{H}^{(a)} \rightarrow {}^{13}\mathrm{C}^{(a)} \rightarrow {}^{13}\mathrm{C}^{(b)} \rightarrow {}^{1}\mathrm{H}^{(b)}$	"HCCH peak"
$(t_1)\ (t_1)\ (t_2)\ (t_3)$	$\Omega(^{13}\mathrm{C}^{(b)}) \pm \Omega(^{1}\mathrm{H}^{(b)})$
	"Diagonal peak"
(4,3)D HC(C)CH	$\Omega(^{13}\mathrm{C}^{(a)}) \pm \Omega(^{1}\mathrm{H}^{(a)})$
$^{1}\mathrm{H}^{(a)} \rightarrow {}^{13}\mathrm{C}^{(a)} \rightarrow {}^{13}\mathrm{C}^{(b)} \rightarrow {}^{13}\mathrm{C}^{(c)} \rightarrow {}^{1}\mathrm{H}^{(c)}$	"HC(C)CH peak"
$(t_1)\ (t_1)\ (t_2)\ (t_3)$	$\Omega(^{13}\mathrm{C}^{(b)}) \pm \Omega(^{1}\mathrm{H}^{(b)})$
	"HCCH Peak"
	$\Omega(^{13}\mathrm{C}^{(c)}) \pm \Omega(^{1}\mathrm{H}^{(c)})$
	"Diagonal Peak"

acquisition, reduction of relaxation delay between scans, or the use of other approaches for non-uniform sampling (e.g. Atreya and Szyperski 2005; Hyberts et al. 2012; Mobli et al. 2012). Finally, the ^{1}H and ^{13}C chemical shifts measured in (4,3)D HC(C)CH/HCCH (Table S2) are in excellent agreement with those previously obtained with the same NMR sample (Gubser and Varani 1996) but from spectra acquired on a different spectrometer: the root-mean-squared-deviation calculated between the previously and newly measured ^{1}H and ^{13}C shifts is only 0.13 and 0.6 ppm, respectively.

Taken together, the (4,3)D HC(C)CH/HCCH based strategy presented here promises to be of high value for efficiently assigning the resonances of larger nucleic acid molecules, including RNA und DNA as well as their protein complexes. In cases of very high shift degeneracy, it may be advantageous to use a similar approach relying on 5D spectral information obtained, for example, from a G^2FT (Atreya et al. 2005) experiment such as (5,3)D {HC}{CC}H.

Table 2 Acquisition parameters of (4,3)D HCCH and HC(C)CH spectra

Experiment	Indirect dimension: t_{max}(ms) Number of complex points Digital resolution (Hz/Pt)[a]	Sub-spectra	Time (h)
(4,3)D HCCH	$\omega_1(^{13}\mathrm{C};\ ^{1}\mathrm{H})$: 6.0(^{13}C)/6.0 (^{1}H); 60; 19.5	$\Omega(^{13}\mathrm{C}) \pm \Omega(^{1}\mathrm{H})$	10
		$\Omega(^{13}\mathrm{C})$	5
	$\omega_2(^{13}\mathrm{C})$: 5.2 (^{13}C); 32; 96	(Central peaks)	
(4,3)D HC(C)CH	$\omega_1(^{13}\mathrm{C};\ ^{1}\mathrm{H})$: 6.0(^{13}C)/6.0 (^{1}H); 58; 20	$\Omega(^{13}\mathrm{C}) \pm \Omega(^{1}\mathrm{H})$	10
		$\Omega(^{13}\mathrm{C})$	5
	$\omega_2(^{13}\mathrm{C})$: 5.2 (^{13}C); 32; 96	(Central peaks)	

[a] Direct dimension $\omega_3(^{1}\mathrm{H})$: 57; 1024; 9

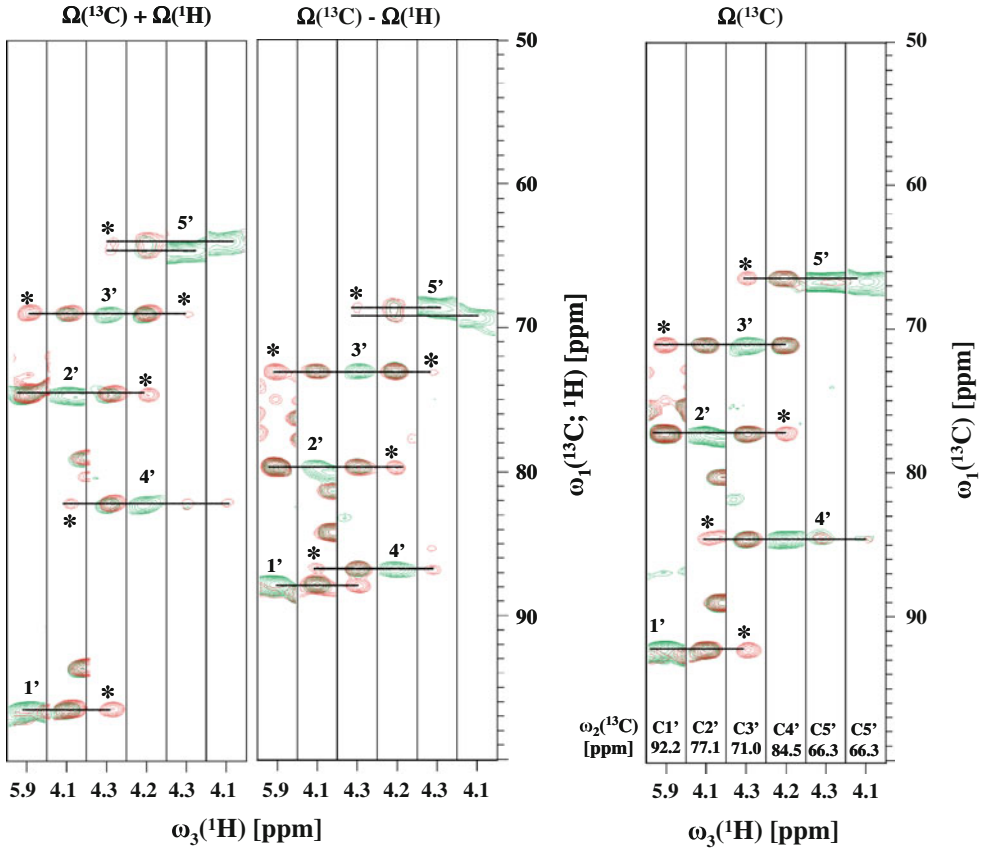

Fig. 4 Superposition of contour plots for [$\omega_1(^{13}C;^{1}H)$,$\omega_3(^{1}H)$]-strips taken from relay (4,3)D HC(C)CH (*peaks in red*) and (4,3)D HCCH (*peaks in green*) spectra recorded at 25 °C and 750 MHz ^{1}H resonance frequency for the 30-nucleotide RNA molecule of Fig. 1. The strips were taken at $\omega_2(^{13}C)$ of G25 and are indicated at the *bottom of the right panel*. The peaks marked with a '*' represent relay peaks observed only in (4,3)D HC(C)CH. The linear combination of shifts observed in a given set of strips is indicated on the *top*. In each strip, the *diagonal peak* is indicated by the *primed number* of the corresponding CH-group, and the *dashed lines* connect peaks belonging to given $^{13}C/^{1}H$ spin system. The low intensity of 'diagonal peaks' in (4,3)D HC(C)CH is due to the fact that delays in the r.f. pulse scheme are tuned for enhancement of the cross peaks (Fig. 3; Table S1). On the *left*, two composite plots of strips are shown taken from the sub-spectra measuring $\Omega(^{13}C) + \Omega(^{1}H)$ and $\Omega(^{13}C)$-$\Omega(^{1}H)$ along the GFT dimension ω_1. On the *right*, a composite plot of strips are shown taken from the 'central peak' 3D (H)C(C)CH (*peaks in red*) and (H)CCH (*peaks in green*) spectra measuring $\Omega(^{13}C)$ along ω_1

Acknowledgments This work was supported by the National Science Foundation (MCB 0817857 to T.S., and MCB 051644 to G.V.), the Department of Science and Technology, India (to H.S.A.), and by the CSIR, India (fellowship to G.J.) We thank Dr. A. Eletski for helpful discussions.

References

Atreya HS, Szyperski T (2004) G-matrix fourier transform NMR spectroscopy for complete protein resonance assignment. Proc Natl Acad Sci USA 101:9642–9647

Atreya HS, Szyperski T (2005) Rapid NMR data collection. Methods Enzymol 394:78–108

Atreya HS, Eletsky A, Szyperski T (2005) Resonance assignment of proteins with high shift degeneracy based on 5D spectral information encoded in G^2FT NMR experiments. J Am Chem Soc 127:4554–4555

Bartels C, Xia TH, Billeter M, Güntert P, Wüthrich K (1995) The program XEASY for computer-supported NMR spectral analysis of biological macromolecules. J Biomol NMR 6:1–10

Batey RT, Inada M, Kujawinski E, Puglisi JD, Williamson JR (1992) Preparation of isotopically labeled ribonucleotides for multidimensional NMR spectroscopy of RNA. Nucleic Acids Res 20:4515–4523

Batey RT, Battiste JL, Williamson JR (1995) Preparation of isotopically enriched RNAs for heteronuclear NMR. Methods Enzymol 261:300–322

Bayer P, Varani L, Varani G (1999) Refinement of the structure of protein-RNA complexes by residual dipolar coupling analysis. J Biomol NMR 14:149–155

Cavanagh J, Fairbrother WJ, Palmer AG, Rance M, Skeleton NJ (2007) Protein NMR spectroscopy. Academic Press, San Diego

Delaglio F, Grzesiek S, Vuister GW, Zhu G, Pfeifer J, Bax A (1995) NMRPipe: a multidimensional spectral processing system based on UNIX pipes. J Biomol NMR 6:277–293

Eletsky A, Atreya HS, Liu G, Szyperski T (2005) Probing structure and functional dynamics of (large) proteins with aromatic rings: L-GFT-TROSY (4,3)D HCCH NMR spectroscopy. J Am Chem 127:14578–14579

Fernández C, Szyperski T, Billeter M, Ono A, Iwai H, Kainosho M, Wüthrich K (1999) Conformational changes of the BS2 operator DNA upon complex formation with the Antennapedia homeodomain studied by NMR with 13C/15N-labeled DNA. J Mol Biol 292:609–617

Grzesiek S, Bax A (1993) Amino acid type determination in the sequential assignment procedure of uniformly $^{13}C/^{15}N$-enriched proteins. J Biomol NMR 3:185–204

Grzesiek S, Kuboniwa H, Hinck AP, Bax A (1995) Multiple-quantum line narrowing for measurement of Ha.-Hb. J couplings in isotopically enriched proteins. J Am Chem Soc 117:5312–5315

Gubser CC, Varani G (1996) Structure of the polyadenylation egulatory element of the uman U1A pre-mRNA 3′-untranslated region and interaction with the U1A protein. Biochem 35:2253–2267

Güntert P (2006) Symbolic NMR product operator calculations. Int J Quantum Chem 106:344–350

Güntert P, Schaefer N, Otting G, Wüthrich K (1993) POMA: a complete Mathematica implementation of the NMR product operator formalism. J Mag Res 101:103–105

Holland DJ, Bostock MJ, Gladden LF, Nietlispach D (2011) Fast multidimensional NMR spectroscopy using compressed sensing. Angew Chem Int Ed Engl 50:6548–6551

Hoogstraten CG, Pardi A (1998) Measurement of carbon-phosphorus J-coupling constants in RNA using spin-echo difference constant-time HCCH-COSY. J Magn Reson 133:236–240

Hyberts SG, Arthanari H, Wagner G (2012) Applications of non-uniform sampling and processing. Top Curr Chem 316:125–148

Kay LE, Keifer P, Saarinen T (1992) Pure absorption gradient enhanced heteronuclear single quantum correlation spectroscopy with improved sensitivity. J Am Chem Soc 114:10663–10665

Kazimierczuk K, Orekhov VY (2011) Accelerated NMR spectroscopy by using compressed sensing. Angew Chem Int Ed Engl 50:5556–5559

Kim S, Szyperski T (2003) GFT NMR, a new approach to rapidly obtain precise high dimensional NMR spectral information. J Am Chem Soc 125:1385–1393

Kojima C, Ono A, Kainosho M (2001) Solid-phase synthesis of selectively labeled DNA: applications for multidimensional nuclear magnetic resonance spectroscopy. Methods Enzymol 338:261–283

Latham MP, Brown DJ, McCallum SA, Pardi A (2005) NMR methods for studying the structure and dynamics of RNA. ChemBioChem 6:1492–1505

Legault P, Jucker FM, Pardi A (1995) Improved measurement of ^{13}C, ^{31}P J coupling constants in isotopically labeled RNA. FEBS Lett 362:156–160

Marino JP, Schwalbe H, Anklin C, Bermel W, Crothers DM, Griesinger C (1994) A three-dimensional triple-resonance ^{1}H, ^{13}C, ^{31}P experiment: sequential through-bond correlation of ribose protons and intervening phosphorus along the RNA oligonucleotide backbone. J Am Chem Soc 116:6472–6473

Masse JE, Bortman P, Dieckmann T, Feigon J (1998) Simple, efficient protocol for enzymatic synthesis of uniformy 13C,15 N-labeled DNA for heteronuclear NMR sudies. Nucleic Acids Res 26:2618–2624

Mobli M, Maciejewski MW, Schuyler AD, Stern AS, Hoch JC (2012) Sparse sampling methods in multidimensional NMR. Phys Chem Chem Phys 21:10835–10843

Nikonowicz EP, Pardi A (1993) An efficient procedure for assignment of the proton, carbon and nitrogen resonances in $^{13}C/^{15}N$ labeled nucleic acids. J Mol Biol 232:1141–1156

Nikonowicz EP, Sirr A, Legault P, Jucker FM, Baer LM, Pardi A (1992) Preparation of ^{13}C and ^{15}N labeled RNA for heteronuclear multidimensional NMR studies. Nucleic Acids Res 20:4507–4513

Pardi A (1992) Isotope labeling for NMR studies of biomolecules. Curr Opin Struct Biol 2:832–835

Price SR, Oubridge C, Varani G, Nagai K (1998) Preparation of RNA-protein complexes for X-ray crystallography and NMR. In: Smith C (ed) RNA-protein interaction: practical approach. Oxford University Press, Oxford, pp 37–74

Ramachandran R, Sich C, Grüne M, Soskic V, Brown LR (1996) Sequential assignments in uniformly 13C- and 15 N-Labelled RNAs: the HC(N, P) and HC(N, P)-CCH-TOCSY experiments. J Biomol NMR 7:251–255

Santoro J, King GC (1992) A constant-time 2D overbodenhausen experiment for inverse correlation of isotopically enriched species. J Magn Reson 97:202–207

Schwalbe H, Marino JP, Glaser SJ, Griesinger C (1995) Measurement of H, H-coupling constants associated with ν1, ν2, and ν3 in uniformly 13C-labelled RNA by HCC-TOCSY-CCH-E.COSY. J Am Chem Soc 117:7251–7252

Shaka AJ, Barker PB, Freeman R (1985) Computer-optimized decoupling scheme for wideband applications and low-level operation. J Magn Reson 64:547–552

Szyperski T, Atreya HS (2006) Principles and applications of GFT projection NMR spectroscopy. Magn Reson Chem 44:S51–S60

Szyperski T, Ono A, Fernández C, Iwai H, Tate S, Wüthrich K, Kainosho M (1997) Measurement of $^{3}JC_{2'P}$ scalar couplings in a 17 kDa protein complex with ^{13}C,^{15}N-labeled DNA distinguishes the B_I and B_{II} phosphate conformations of the DNA. J Am Chem Soc 119:9901–9902

Szyperski T, Fernández C, Ono A, Kainosho M, Wüthrich K (1998) Measurement of deoxyribose $^{3}J_{HH}$ scalar couplings reveals protein binding-induced changes in the sugar puckers of the DNA. J Am Chem Soc 120:821–822

Szyperski T, Fernández C, Ono A, Wüthrich K, Kainosho M (1999) The 2D 31P spin-echo-difference constant-time [13C, 1H]-HMQC experiment for simultaneous determination of 3JH3′P and 3JC4′P in 13C-labeled nucleic acids and their protein complexes. J Magn Reson 140:491–494

Szyperski T, Yeh DC, Sukumaran DK, Moseley HNB, Montelione GT (2002) Reduced-dimensionality NMR spectroscopy for high-throughput protein resonance assignment. Proc Natl Acad Sci USA 99:8009–8014

Varani G, Tinoco I Jr (1991) RNA structure and NMR spectroscopy. Q Rev Biophys 24:479–532

Varani G, Aboul-ela F, Allain FH-T, Gubser CC (1995) Novel three-dimensional 1H–13C-31P triple resonance experiments for sequential backbone correlations in nucleic acids. J Biomol NMR 5:315–320

Varani G, Aboul-ela F, Allain FH-T (1996) NMR investigations of RNA structure. Progr NMR Spectrosc 29:51–127

Vuister GW, Bax A (1992) Resolution enhancement and spectral editing of uniformly 13C enriched proteins by homonuclear broadband 13C–13C decoupling. J Magn Reson 98:428–435

Wu Z, Delaglio F, Tjandra N, Zhurkin VB, Bax A (2003) Overall structure and sugar dynamics of a DNA dodecamer from homo- and heteronuclear dipolar couplings and 31P chemical shift anisotropy. J Biomol NMR 26:297–315